Identification of Potent Nontoxic Poly(ADP-Ribose) Polymerase-1 Inhibitors: Chemopotentiation and Pharmacological Studies[1]

Christopher R. Calabrese, Michael A. Batey, Huw D. Thomas, Barbara W. Durkacz, Lan-Zhen Wang, Suzanne Kyle, Donald Skalitzky, Janke Li, Catherine Zhang, Theodore Boritzki, Karen Maegley, Alan H. Calvert, Zdenek Hostomsky, David R. Newell, and Nicola J. Curtin[2]

Northern Institute for Cancer Research, The University of Newcastle upon Tyne, Medical School, Newcastle upon Tyne, NE2 4HH, United Kingdom [C. R. C., M. A. B., H. D. T., B. W. D., L-Z. W., S. K., A. H. C., D. R. N., N. J. C.], and Pfizer Global Research and Development/Agouron Pharmaceuticals, Inc., La Jolla, California [D. S., J. L., C. Z., T. B., K. M., Z. H.]

ABSTRACT

The nuclear enzyme poly(ADP-ribose) polymerase (PARP-1) facilitates DNA repair, and is, therefore, an attractive target for anticancer chemo- and radio-potentiation. Novel benzimidazole-4-carboxamides (BZ1–6) and tricyclic lactam indoles (TI1–5) with PARP-1 K_i values of <10 nM have been identified.

Whole cell PARP-1 inhibition, intrinsic cell growth inhibition, and chemopotentiation of the cytotoxic agents temozolomide (TM) and topotecan (TP) were evaluated in LoVo human colon carcinoma cells. The acute toxicity of the inhibitors was investigated in PARP-1 null and wild-type mice. Tissue distribution and *in vivo* chemopotentiation activity was determined in nude mice bearing LoVo xenografts.

At a nontoxic concentration (0.4 μM) the PARP-1 inhibitors potentiated TM-induced growth inhibition 1.0–5.3-fold and TP-induced inhibition from 1.0–2.1-fold. Concentrations of the PARP-1 inhibitors that alone inhibited cell growth by 50% ranged from 8 to 94 μM. Maximum potentiation of TM activity was achieved at nongrowth inhibitory concentrations (≤1 μM) of potent PARP-1 inhibitors BZ5 and TI4. Whole cell PARP-1 inhibition by BZ3, BZ5, BZ6, TI1, and TI4 was confirmed by attenuation of DNA damage-induced NAD^+ depletion. Selected inhibitors (TI1, TI3, and TI4), in contrast to the benchmark compound PD128763, caused only mild hypothermia in both PARP-1 null and wild-type mice. Excellent distribution of BZ5, TI1, and TI3 into tumor tissue was observed, and TI3 enhanced TM antitumor activity *in vivo*.

These studies have identified potent nontoxic PARP-1 inhibitors with structural modifications that promote aqueous solubility, tolerability, and tissue distribution. These compounds are important leads in the development of clinically viable PARP-1 inhibitors.

INTRODUCTION

The abundant nuclear enzyme PARP-1[3] (EC 2.4.2.30) is a major research focus in the fields of cancer, diabetes, and ischemia-reperfusion injury. PARP-1 is a M_r 116,000 enzyme that comprises a NH_2-terminal DNA-binding domain containing two zinc fingers that recognize DNA strand breaks, an automodification domain, and a COOH-terminal catalytic domain (1). PARP-1 is the founder and best characterized member of a family of enzymes largely associated with the maintenance of genomic stability (2, 3). Activation of PARP-1 is part of the immediate cellular response to DNA strand breaks. PARP-1 catalyzes the cleavage of NAD^+ to synthesize long linear or branched homopolymers of ADP-ribose on nuclear proteins, primarily PARP-1 itself and histones, with the release of nicotinamide (4–7). The ADP-ribose polymers are degraded by poly(ADP-ribose) glycohydrolase (8, 9) such that the rapid turnover of ADP-ribose polymers after DNA damage can result in severe acute NAD^+ depletion (10).

PARP-1 activation after DNA damage has pleiotropic functions, including promotion of DNA repair (11, 12), modulation of p53 interactions (13, 14), and regulation of apoptosis (15, 16). Evidence for involvement in DNA repair is extensive, and PARP-1 is a component of the DNA base excision repair multiprotein complex comprising PARP-1, DNA ligase III, XRCC, and DNA polymerase β (17). The activation of PARP-1 by, and involvement of PARP-1 in the repair of, DNA strand breaks prompted investigations into the effect of PARP-1 inhibition on DNA-damaging anticancer therapies. These investigations have used gene disruption (18–21) and other molecular and genetic approaches (22–26), as well as the development of small molecule inhibitors of the enzyme (27, 28). Promising *in vitro* studies with the early substituted benzamide PARP-1 inhibitors (*e.g.*, 3-aminobenzamide; Refs. 29–31) prompted additional inhibitor development to improve potency and selectivity. Subsequent studies identified the dihydroisoquinolinone, PD128763, the quinazolin-4-(3*H*)-one,

Received 12/10/02; revised 3/6/03; accepted 3/13/03.
The costs of publication of this article were defrayed in part by the payment of page charges. This article must therefore be hereby marked *advertisement* in accordance with 18 U.S.C. Section 1734 solely to indicate this fact.
[1] Supported by Pfizer Global Research and Development/Agouron Pharmaceuticals, Inc., La Jolla, CA, and by Cancer Research-United Kingdom.
[2] To whom requests for reprints should be addressed, at Northern Institute for Cancer Research, The University of Newcastle upon Tyne, Medical School, Framlington Place, Newcastle upon Tyne, NE2 4HH, United Kingdom. Phone: 191-222-7133; Fax: 191-222-7556; E-mail: n.j.curtin@ncl.ac.uk.

[3] The abbreviations used are: PARP, poly(ADP-ribose) polymerase; TM, temozolomide; TP, topotecan; HPLC, high-performance liquid chromatography; GI_{50}, concentration of drug required to inhibit cell growth by 50%; PF_{50}, potentiation factor; MNNG, *N*-methyl-*N*'-nitro-*N*-nitrosoguanidine; RTV, relative tumor volume.

Table 1 Inhibition of PARP-1, LoVo cell growth, and chemosensitization by PARP-1 inhibitors

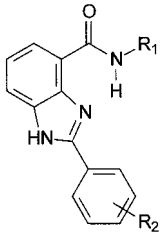

Benzimidazole series

Compound	R_1	R_2	K_i[a] (nM)	GI_{50}[b] (μM)	TM PF_{50}[c]	TP PF_{50}
NU1085	H	4′-OH	6	94 ± 11	>1.8[d]	4[d]
BZ1	CH_3	4′-OCH_3	>1000	8	0.9 ± 0.2	1.1 ± 0.1
BZ2	H	4′-OCH_3	2.5	75, 74	1.5 ± 0.3[e]	1.0 ± 0.1
BZ3	H	4′-CI	6.5	62 ± 12	1.5 ± 0.3[e]	1.2 ± 0.2
BZ4	H	2′-CI	9	53	1.2 ± 0.1	1.2 ± 0.4
BZ5	H	4′-$CH_2N(CH_3)_2$	4.5	43 ± 3	4.0 ± 1.0[e]	1.5 ± 0.4[e]
BZ6	H	3′-$CH_2N(CH_3)_2$	7.5	64 ± 5	1.7 ± 0.1[e]	1.5 ± 0.3[e]

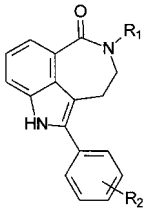

Tricyclic Lactam Indole series

TI1	H	4′-H	4.1	52 ± 9	1.9 ± 0.7[e]	2.1 ± 0.4[e]
TI2	H	4′-CI	4.1	11 ± 3	1.8 ± 0.3[e]	1.4 ± 0.4
TI3	H	4′-F	4.2	20 ± 5	1.7 ± 0.5[e]	1.9 ± 0.3[e]
TI4	H	4′-$CH_2N(CH_3)_2$	5.0	9 ± 0.3	5.3 ± 1.5[e]	1.9 ± 0.3[e]
TI5	H	3′-$CH_2N(CH_3)_2$	7.5	22 ± 6	4.5 ± 0.8[e]	2.0 ± 0.3[e]

[a] K_i values were determined using recombinant human PARP-1.
[b] GI_{50} values for the compounds were determined after 5-day exposure of LoVo cells by SRB.
[c] PF_{50} = Potentiation of TM and TP at GI_{50}. Data are individual values or mean ± SD of four independent experiments.
[d] Data from Delaney *et al.* Ref. 33.
[e] GI_{50} for combination significantly different from TM or TP alone (paired, two-tailed Student's *t* test).

NU1025, and the benzimidazole-4-carboxamides NU1064 and NU1085 as more potent PARP-1 inhibitors (32, 33). Both NU1025 and NU1085 demonstrated significant potentiation of growth inhibition and cytotoxicity induced by TM (a monofunctional DNA alkylating agent) and TP (a topoisomerase I inhibitor) in a panel of human tumor cell lines *in vitro* (33). PD128763 was shown to potentiate the antitumor activity of ionizing radiation both *in vitro* and *in vivo*, and the activity of methylating agents *in vitro* (34, 35).

Both X-ray crystallographic studies of inhibitors bound to the active site of PARP-1 (36, 37) and structure-activity relationships (32) demonstrate that potent PARP-1 inhibition is dependent on the orientation of the carboxamide oxygen to form three hydrogen bonds with Ser-904 and Gly-863 in the PARP-1 NAD^+ binding site. Analysis of the binding of the benzimidazole, NU1085, demonstrated a large pocket that can accommodate a number of substitutions (37). Using a rational drug design approach, based on crystallographic data, a number of benzimidazoles and tricyclic lactam indoles were developed in which the carboxamide group was maintained in the favorable orientation by intramolecular hydrogen bonding as in benzimidazole inhibitors (38), or incorporation into a seven-membered ring as in tricyclic lactam indole inhibitors (Ref. 39; Table 1). The aim of the studies presented here was to use representative examples of benzimidazole and tricyclic lactam indole PARP-1 inhibitors to evaluate the effects of substitutions consistent with enzyme inhibitory activity in relation to *in vitro* activity (chemopotentiation), solubility, tissue distribution, and antitumor activity in preclinical *in vitro* and *in vivo* studies.

MATERIALS AND METHODS

TM (a gift from the Cancer Research-UK, London, United Kingdom) and TP (SmithKline Beecham Pharmaceuticals, Philadelphia, PA) were dissolved in DMSO at 10 and 2.2 mM, respectively, and stored at −20°C. Benzimidazole-4-carboxamide PARP-1 inhibitors BZ1–6 and TI1–5 were synthesized as described previously in (38)[4] and (39), respectively. Stock so-

[4] A. H. Calvert, N. J. Curtin, B. T. Golding, R. J. Griffin, Z. Hostomsky, R. A. Kumpf, J. Li, K. Maegley, D. R. Newell, D. Skalitsky, A. W. White. A novel series of benzimidazole PARP-1 inhibitors that potentiate cytotoxic drugs in human tumour cell lines, manuscript in preparation.

lutions, prepared in DMSO at 100 mM, were stored at −20°C. Drugs (alone or in combination) were added to cell cultures so that final DMSO concentrations were consistently 1% (v/v). Solvents (HPLC grade) for HPLC analysis were obtained from Fisher Scientific Ltd. (Loughborough, United Kingdom). All of the other chemicals and reagents were supplied by Sigma (Poole, United Kingdom) unless otherwise stated.

PARP-1 Inhibition Assays. PARP-1 activity *in vitro* was measured using 20 nM full-length recombinant human PARP-1, 500 μM NAD^+ + [^{32}P]NAD^+ (0.1–0.3 μCi/reaction), and 10 μg/ml activated calf thymus DNA. ^{32}P incorporation into polymer was quantified using a PhosphorImager (Molecular Dynamics) as described previously (40). K_is were calculated by nonlinear regression analysis.

Cell Growth Inhibition Assays. LoVo colorectal cancer cells (American Type Culture Collection, Manassas, VA) were maintained as exponentially growing monolayers in RPMI 1640 supplemented with 10% (v/v) FCS, 1000 units/ml penicillin, and 100 μg/ml streptomycin (Life Technologies, Inc., Paisley, United Kingdom). Cells were evaluated every 4–8 weeks to exclude *Mycoplasma* contamination (41).

Exponentially growing cells in 96-well plates were exposed to single agent TM, TP, PARP-1 inhibitor, or drug combinations (6 replicates per drug treatment) for 5 days. Controls were cells exposed to 1% (v/v) DMSO, cytotoxic drug, or PARP-1 inhibitors alone. At the time drugs were added, replicate wells were fixed to estimate cell number at the initiation of drug incubations. At the end of the exposure period, cells were fixed, stained with sulforhodamine B (42), and the absorbance at 570 nm was measured (Dynatech MR7000; Dynatech, Billinghurst, United Kingdom). Cell growth was calculated as a percentage of the appropriate control, and growth inhibitory GI_{50} values were calculated from computer-generated growth inhibition curves (GraphPad Software, Inc., San Diego, CA). The PF_{50} was calculated as the ratio GI_{50} cytotoxic drug alone:GI_{50} cytotoxic drug plus PARP-1 inhibitor combination.

Measurement of NAD^+ Depletion after PARP-1 Activation in Intact Cells. LoVo cells were exposed to 25 μM of the DNA methylating agent MNNG for 60 min to activate PARP-1 in the presence or absence of 0.4 μM of the PARP-1 inhibitors BZ3, BZ5, BZ6, TI1, and TI4 (Table 1) after which NAD^+ content was determined by colorimetric assay as described previously (43). Data are expressed as a percentage of the NAD^+ content of untreated control cells.

Analysis of PARP-1 Inhibitor Concentrations in Biological Samples. NU1085 was separated on a Waters Alliance 2780 separation module (Waters, Watford, United Kingdom) using a Genesis 4 μm C18 column (4.6 × 100 mm; Jones Chromatography Ltd., Mid Glamorgan, United Kingdom) and a mobile phase of sodium acetate buffer (0.1 M; pH 5) and acetonitrile (75:25; v/v) at a flow rate of 1 ml/min. Detection was via UV absorption (329 nm; PDA 996 detector; Waters). Separation of BZ5 was achieved on a Phenomenex Prodigy 5 ODS2 column (3.2 × 150 mm; Phenomenex United Kingdom, Macclesfield, United Kingdom) using a mobile phase of 0.1% (w/w) ammonium formate buffer (pH 6.0) and acetonitrile (85.5:14.5; v/v) at a flow rate of 0.8 ml/min. TI1 and TI3 were separated using a Hypersil BDS 5 μm column (4.6 × 250 mm; Jones Chromatography) with a mobile phase of 0.1% (w/v) ammonium formate buffer (pH 7.0) and acetonitrile (60:40; v/v), and detected at 345 nm. Extraction from biological tissues (liver, brain, and tumor), homogenized in saline (0.15 M NaCl; 1:3 w/v tissue to saline), was performed using protein precipitation with acetonitrile (1:4 v/v) followed by centrifugation (5000 × *g* at room temperature), evaporation of the supernatant to dryness under nitrogen at 30°C, and reconstitution in mobile phase before analysis. Standard curves for each PARP-1 inhibitor, prepared in plasma, were linear over the range 0.2–20 μg/ml ($r^2 > 0.998$) with triplicate QA standards (at 0.2, 10, and 20 μg/ml) showing intra- and interassay variation of <10%. Tissue concentrations were calculated using the method of addition (44) to compensate for intersample variation. Concentrations were calculated from the resultant standard curves (r^2 values > 0.99). Tissue concentrations are expressed normalized to dose [μM/(50 mg/kg dose)].

Tissue Distribution. All of the *in vivo* experiments were reviewed and approved by the relevant institutional animal welfare committees, and performed according to national law. Female athymic nude mice (CD1 *nu/nu*, Charles River) used for tissue distribution studies were maintained and handled in isolators under specific pathogen-free conditions. Tumors were generated by implantation of LoVo colorectal tumor cells s.c. into the flanks of CD-1 nude mice (1×10^7 cells/animal). Tissue distribution studies were performed when tumors had reached a size of ~650 mm^3 (10–14 days after implantation). NU1085 and TI3 were administered as single i.p. doses (at 40 or 50 mg/kg, respectively, limits of solubility in vehicle) in 40% (v/v) PEG 300 (polyethylene glycol, av. mol. wt. 285–315) in sterile saline. TI1 was delivered in a vehicle of 20% hydroxypropyl β-cyclodextrin in sterile saline at 50 mg/kg i.p.

The *N*,*N*-dimethyl aminomethyl substituted benzimidazole BZ5 was readily soluble as the HCl salt and administered as a single 50 mg/kg i.p. dose in sterile saline. At 30 and 60 min after treatment, LoVo xenograft-bearing mice (4/time point) were anesthetized (0.75 mg/kg fentymal citrate, 25 mg/kg fluanisone, and 12.5 mg/kg midazolam, i.p.) and blood removed by cardiac puncture. Animals were then killed and tissues (liver, tumor, and brain) removed, frozen in liquid nitrogen, and stored at −80°C. Tissues were homogenized in 3 volumes of saline and analyzed by HPLC as above.

Acute Toxicity of the PARP-1 Inhibitors *in Vivo*. PARP-1 knockout and wild-type mice used for toxicity studies were from a colony of animals derived from those generated by Menissier-de Murcia *et al.* (19). Animals were treated with TI1 (50 or 100 mg/kg i.p.), TI3 (50 mg/kg i.p.), TI4 (100 mg/kg i.p.), or PD128763 (25 or 50 mg/kg i.p.). TI4 was readily soluble as the HCl salt and administered in sterile saline. PD128763 was administered in a vehicle of 10% dimethyl acetamide in sterile saline. Body temperatures were monitored using a Testo 925 rectal probe (Testo, Hampshire, United Kingdom) before (T0) and after treatment (up to 8.5 h) with a final measurement at 24 h after treatment.

Determination of Antitumor Activity *in Vivo*. CD-1 nude mice bearing LoVo colorectal cancer xenografts s.c. (n = 5/group) were treated when tumors were palpable (10–12 days after implantation). Control animals were treated with normal saline (for 5 days). TM was administered p.o. at 68 mg/kg/day (for 5 days) either alone or in combination with TI3 adminis-

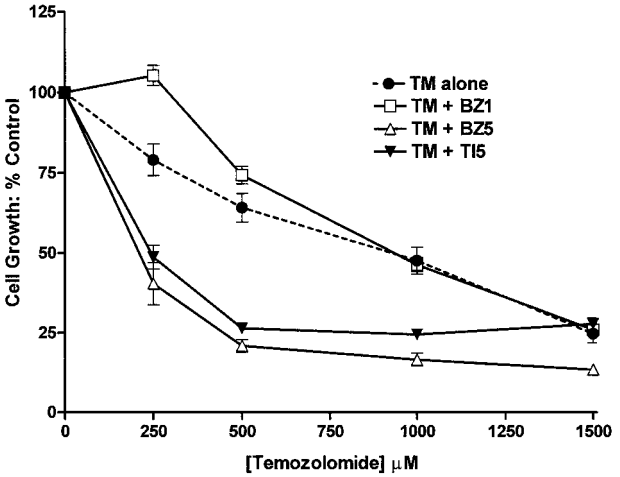

Fig. 1 Potentiation of TM-induced growth inhibition by selected benzimidazole and tricyclic lactam indole PARP-1 inhibitors. LoVo cell growth was determined by SRB assay after 5-day exposure to TM alone (●), TM in the presence of 0.4 μM of the PARP-1 inhibitors BZ5 (△), or TI5 (▼) or the inactive control compound BZ1 (□) as described in "Materials and Methods." Data are mean of four independent experiments, normalized to 1% DMSO or 0.4 μM PARP-1 inhibitor, as appropriate; *bars*, ±SD.

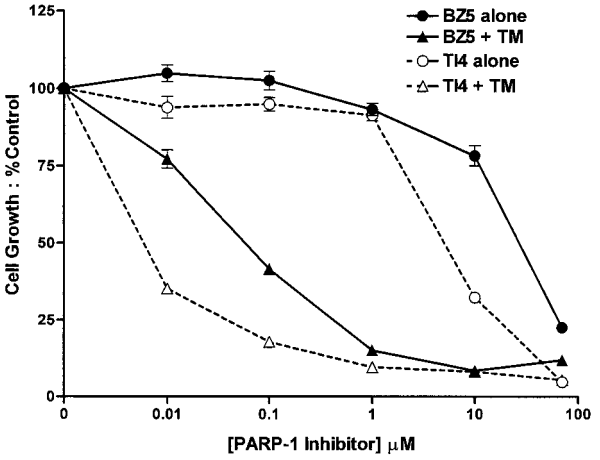

Fig. 2 Effect of PARP-1 inhibitors BZ5 and TI4 on the growth inhibitory effect of a subcytotoxic TM concentration in LoVo cells. Growth inhibition was determined by the SRB assay after a 5-day exposure to BZ5 alone (●), TI4 alone (○), BZ5 + 400 μM TM (▲), TI4 + 400 μM TM (△). TM (400 μM) alone inhibits growth by ~20%. Data are mean (three independent experiments) normalized to1% DMSO or 400 μM TM, as appropriate; *bars*, ±SD.

tered at 50 mg/kg/day i.p. (for 5 days) in a vehicle of 40% PEG 300) in sterile saline. Two-dimensional caliper measurements were made and tumor volume calculated using the equation $a^2 \times b/2$, where a is the smallest measurement and b the largest. Data are presented as median RTV, where the tumor volume on the initial day of treatment (day 0) is assigned an RTV value of 1.

RESULTS

***In Vitro* PARP-1 Inhibition and Chemosensitization.** Measurement of the activity of NU1085, BZ2–6, and TI1–5 against purified human PARP-1 indicated potent inhibition with all of the compounds (K_i values in the range 2.5–9 nM; Table 1). The control compound BZ1, which, by virtue of the *N*-methyl substituent cannot form a hydrogen bond with Gly-863 of the target enzyme (38), was inactive, as predicted (Table 1). There was a 10-fold variation of the growth inhibitory activity of the PARP-1 inhibitors alone in LoVo cells (GI_{50} values ranged from 8 to 94 μM), which was not related to PARP-1 inhibitory potency; *i.e.*, BZ1 was among the most growth inhibitory compounds yet inactive as a PARP-1 inhibitor (Table 1).

To study PARP-1 inhibitor-mediated chemosensitization a fixed nongrowth inhibitory PARP-1 inhibitor concentration of 0.4 μM (<5% of the GI_{50} for the inhibitor alone) was used. We have shown previously that potentiation of TM- and TP-induced growth inhibition is in good agreement with the potentiation of their cytotoxicity (clonogenic survival) by the quinazolinone PARP-1 inhibitor NU1025 and the benzimidazole, NU1085, in a panel of 12 human tumor cell lines (33). Representative LoVo growth inhibition curves for TM in combination with the inactive control compound, BZ1, and potent inhibitors, BZ5 and TI5, are shown in Fig. 1, and mean PF_{50} values (for combinations with either TM or TP) calculated from four independent experiments are given in Table 1. The compounds exhibited a spectrum of activity for TM and TP potentiation with PF_{50} values (Table 1) ranging from 1.0 to 5.3, variation that was not related to their inherent growth inhibitory potency (GI_{50}). BZ5, TI4, and TI5 produced the greatest TM potentation. As expected, the inactive PARP-1 inhibitor BZ1 did not potentiate the activity of either TM or TP in LoVo cells.

Additional studies were performed with BZ5 and TI4 to determine the minimum concentration required to achieve maximum potentiation of a fixed concentration of TM (*i.e.*, 400 μM, which on its own inhibits cell growth by ~20%). Increasing potentiation of TM was observed with increasing concentrations of both compounds. Maximum potentiation was observed with PARP-1 inhibitor concentrations of 1 μM or less, which increased the growth inhibitory activity of TM from 20% to 85% (Fig. 2). These PARP-1 inhibitor concentrations represent <5% of the IC_{50} concentrations and were not growth inhibitory *per se* (<10% growth inhibition).

To determine the ability of the compounds to inhibit PARP-1 activity in whole cells, NAD^+ depletion after MNNG-induced PARP-1 activation was examined. Exposure of LoVo cells to the methylating agent MNNG (25 μM) caused cellular NAD^+ pools to be reduced to below the detection limit (0.5 nmol/ml) within 60 min. In the presence of 0.4 μM BZ3, BZ5, BZ6, TI1, or TI4, the depletion of NAD^+ was attenuated such that 24–60% of the pretreatment concentration remained at 60 min (Fig. 3).

***In Vivo* Tissue Distribution.** On the basis of the above *in vitro* data, a number of compounds (BZ5, TI1, and TI3) were selected for tissue distribution studies in comparison to the parent compound, NU1085, in LoVo xenograft-bearing CD-1 nude mice (Fig. 4, *A* and *B*). Only limited distribution of NU1085 into both tumor and brain tissue was observed. In contrast, at 30 min the tumor concentration of the *N*,*N*-dimeth-

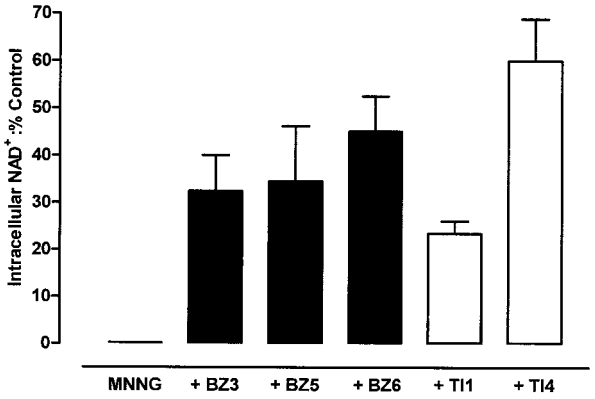

Fig. 3 Prevention of MNNG-induced NAD^+ depletion by selected PARP-1 inhibitors. Cellular NAD^+ content was measured in LoVo cells exposed to 25 μM MNNG for 60 min in the presence or absence of 0.4 μM BZ3, BZ5, BZ6 (■), TI1 or TI4 (□). Data, calculated as percentage of untreated control, are mean of three independent experiments; *bars*, ±SD.

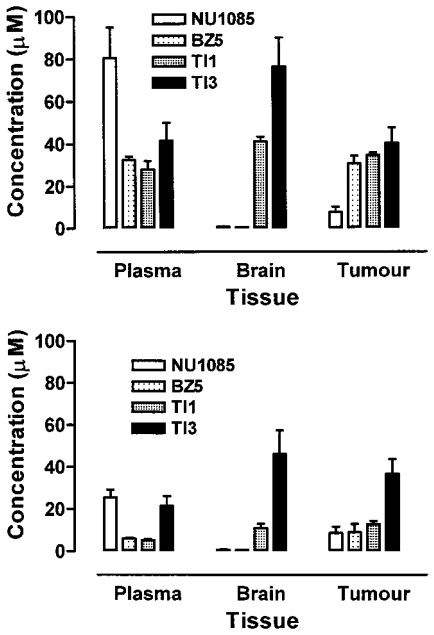

Fig. 4 Tissue distribution of selected PARP-1 inhibitors. Plasma and tissue concentrations of NU1085, BZ5, TI1, and TI3 were determined in LoVo xenograft bearing CD-1 nude mice at (*A*) 30 and (*B*) 60 min after treatment. Doses were 50 mg/kg i.p. (BZ5, TI1, and TI3) or 40 mg/kg i.p. (NU1085). Data presented as mean (n = 4 animals/time point); data for NU1085 have been normalized to a dose of 50 mg/kg to allow comparison; *bars*, ±SE.

ylaminomethyl substituted benzimidazole BZ5 was 4-fold higher than achieved with NU1085 despite lower plasma concentrations than NU1085, although there was no improvement in distribution into brain tissue. The 4′-fluorinated tricyclic lactam indole, TI3, and its parent compound, TI1, both showed extensive distribution into tumor and brain at 30 min. Tissue:plasma ratios (Table 2) suggested retention of all of the compounds within tumor tissue over the period of the study. At 60 min after administration, the tumor concentrations of BZ5, TI1, and TI3 were 9.0, 12.9, and 36.9 μM, respectively, from a 50 mg/kg dose. This represents tumor concentrations 22–93-fold greater than that required for chemopotentiation *in vitro* (0.4 μM).

Table 2 Tissue distribution of selected PARP-1 inhibitors

Tissue:plasma ratios were calculated from distribution data (as described in Fig. 4) after i.p. administration of NU1085 (40 mg/kg), BZ5, TI1, and TI3 (50 mg/kg).

		Tissue:Plasma ratio			
Time	Tissue	NU1085	BZ5	TI1	TI3
30 min	Brain	0.01	0	1.5	1.8
	Tumor	0.1	1.0	1.2	1.0
	Liver	2.3	5.6	3.9	3.9
60 min	Brain	0.03	0	2.1	2.1
	Tumor	0.34	1.5	2.4	1.7
	Liver	2.9	5.2	6.6	5.2

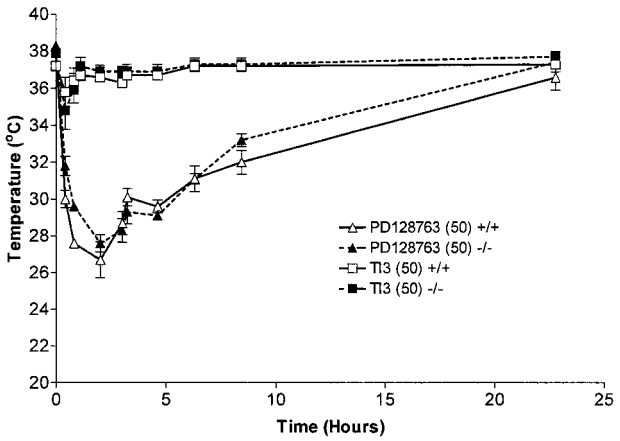

Fig. 5 Effect of PD128763 and TI3 on the body temperature of PARP-1 wild-type and knockout mice. PARP-1 wild type (■, △) and knockout mice (■, ▲; n = 3/group) were treated with either TI3 (50 mg/kg i.p.) (□, ■) or PD128763 (50 mg/kg i.p.; △, ▲), and body temperatures monitored up to 24 h after treatment; *bars*, ±SD.

Acute Toxicity. In the tissue distribution studies all of the compounds studied were well tolerated at the doses used. Potential acute toxicity was additionally evaluated using PARP-1 knockout and wild-type mice in direct comparison with the isoquinolinone PARP-1 inhibitor PD128763 (Fig. 5; Table 3). The acute toxic sequela of PD128763 administration was profound hypothermia, at doses of 25 and 50 mg/kg. Equivalent toxicity was observed in wild-type and PARP-1 knockout animals indicating the toxicity to be a PARP-1 independent event. The tricyclic lactam indoles TI1, TI3, and TI5, which are 10 times more potent PARP-1 inhibitors than PD128763 (K_i = 85 nM) were much less toxic despite administration of molar doses equivalent to, or in excess of, PD128763.

***In Vivo* Chemosensitization.** Compound TI3 was selected for *in vivo* chemosensitization studies by virtue of its lack of toxicity (Fig. 5), and its good tumor and brain penetration and

Table 3 Summary of nadir body temperature measurements after treatment of PARP-1 wild-type and knockout mice with selected PARP-1 inhibitors

Body temperature measured at 25-min intervals for the first 5 h and 60-min intervals thereafter i.p. administration of PARP-1 inhibitor at doses presented as both mg/kg and {mol/kg}. Representative data for TI3 and PD128763 are shown in Fig. 5. Temperatures are presented as mean ± SD (n = 3 animals per group).

Compound	Dose (mg/kg) {μmols/kg}	Nadir body temp (°C) (mean ± SD)		Nadir time (min)	
		+/+	−/−	+/+	−/−
Control	−	37 ± 1	37 ± 1	−	−
PD128763	25 {155}	32 ± 1	31 ± 1	120	120
	50 {310}	27 ± 2	28 ± 1	120	120
TI1	50 {190}	33 ± 1	34 ± 1	20	20
	100 {380}	30 ± 1	30 ± 1	50	50
TI3	50 {178}	36 ± 1	35 ± 2	50	25
TI4	100 {312}	34 ± 1	33 ± 1	25	25

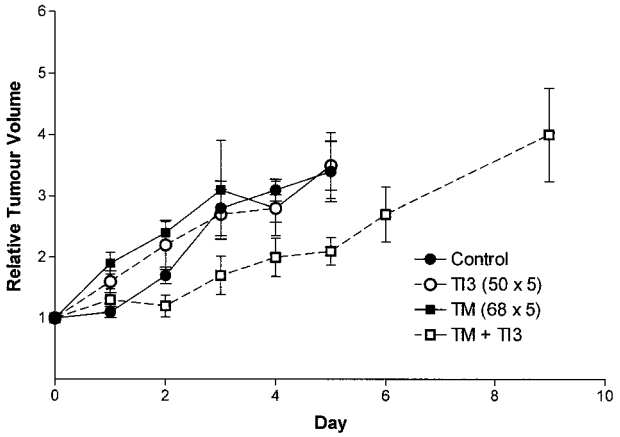

Fig. 6 Antitumor activity of TI3 in combination with TM. CD-1 nude mice bearing LoVo colorectal cancer xenografts s.c. (n = 5/group) were treated when tumors were palpable (10–12 days after implantation). TM (68 mg/kg/day p.o.) or TI3 (50 mg/kg/day i.p.) were administered either alone or in combination (days × 5). Control animals were treated with normal saline (days × 5). Two-dimensional caliper measurements were made and RTV calculated; *bars*, ±SD.

retention (Fig. 4). Nude mice bearing LoVo xenografts received either TI3 (50 mg/kg i.p.) or TM (68 mg/kg p.o.) alone or in combination daily for 5 days. Neither TI3 or TM alone significantly inhibited tumor growth (median times to RTV3 of 5 days for both treatments). However, combination of the two agents significantly ($P < 0.01$) increased the time to reach RTV3 to a median of 9 days (Fig. 6).

DISCUSSION

PARP-1 is an important target for therapeutic intervention in common human disorders such as cancer, diabetes, stroke, and other ischemia-reperfusion injury (45). However, the preclinical development of PARP-1 inhibitors as potential adjuvants to anticancer therapy has been limited by lack of potency and favorable pharmacological properties (27). Selected potent novel benzimidazole and tricyclic lactam indole PARP-1 inhibitors, developed using crystal-based drug design, were evaluated *in vitro* and *in vivo* in the current study. In addition, the *N*-methyl substituted negative control compound, BZ1, was synthesized and shown to be inactive as a PARP-1 inhibitor and chemopotentiator, confirming that hydrogen bonding to Gly-863 is important to activity as proposed previously (27). Several modifications, predicted from earlier studies to be associated with potent PARP-1 inhibition (38), were made to the pendant phenyl ring to investigate chemopotentiation, solubility, and tissue distribution. The compounds varied in their ability to increase the activity of the cytotoxic agents TM and TP against LoVo human colon cancer cells *in vitro*, with BZ5, TI4 and TI5 being particularly active. In general, a greater potentiation of TM was observed compared with TP in this tumor cell line. There was no clear correlation between the activity of the compounds as inhibitors of purified PARP-1 and their ability to potentiate TM- or TP-induced growth inhibition in the cell lines studied. Hence, other factors, notably cellular uptake and retention, may be significant determinants of cellular activity. To confirm that the whole cell activity of these novel compounds was related to inhibition of PARP-1, prevention of NAD^+ depletion induced by the potent methylating agent MNNG was used as a surrogate marker for PARP-1 activity. All of the compounds studied (BZ3, BZ5, BZ6, TI1, and TI4) attenuated the depletion of cellular pools of NAD^+ confirming PARP-1 inhibition in viable cells. Notably, TI4, one of the compounds with the greatest activity in the chemosensitization assays, produced the greatest inhibition of NAD^+ depletion.

The growth inhibitory activity of the tricyclic indoles alone was about 3–4-fold greater than that of the benzimidazoles, despite equivalent PARP-1 inhibitory potency and TM or TP potentiation, suggesting a compound class effect rather than a PARP-1-mediated effect. Notably, the inactive control BZ1 was more growth inhibitory than the active benzimidazole inhibitors (NU1085 and BZ2–6) suggesting that weak growth inhibition can be observed with this structural class but that PARP-1 inhibition is not the underlying mechanism. Importantly, maximum potentiation of a low concentration of TM by BZ5 and TI4 was observed at PARP-1 inhibitor concentrations of 1 μM or less, <5% of the GI_{50} for these PARP-1 inhibitors alone. As such, chemosensitization was achieved at concentrations that are nontoxic, an important criterion to be satisfied by resistance-modifying agents.

The promising activity of a number of these compounds *in vitro* prompted additional investigation *in vivo*. To date, the *in vivo* evaluation of inhibitors of PARP-1 has been limited, particularly in the field of anticancer therapeutics. Initial investigations *in vivo* with PD128763 have not been pursued, possibly because of adverse toxicity and pharmacological properties, notably hypothermia. The tricyclic lactam indole compounds investigated here caused only modest acute toxic effects (hypothermia) that were similar in both wild-type and PARP-1 knockout animals. Together with the observation that the compounds were >10 times more potent PARP-1 inhibitors than PD128763, yet at equimolar concentrations caused less toxicity, these data demonstrate that hypothermia is not PARP-1 inhibition related.

Incorporation of solublizing substitutions into both the benzimidazole and tricyclic lactam indole classes of PARP-1

inhibitors improved aqueous solubility without compromising their potency against the target enzyme or *in vitro* activity. Furthermore, in the tricyclic lactam series, the 4′F derivative, TI3, gave excellent and sustained tumor and brain drug concentrations.

In vivo chemopotentiation of TM in the refractory LoVo tumor xenograft by TI3, selected because of its good tumor penetration and lack of acute toxicity, was significant but modest, and additional analogue development is continuing with the aim of combining good pharmacological properties with potent *in vitro* chemosensitizing activity (46)

In conclusion, potent novel PARP-1 inhibitors have been identified that significantly increase the growth inhibitory activity of TM and TP in human colon cancer cell lines *in vitro* at nM concentrations that are nontoxic *per se*. Administration of the inhibitors to mice resulted in tumor levels that should, on the basis of *in vitro* data, be active in combination studies with anticancer chemotherapeutics. Moreover, no acute toxicity was observed with these compounds. These encouraging data are being used to drive additional analogue development for *in vivo* antitumor studies in combination with clinically relevant antitumor therapies.

REFERENCES

1. Kameshita, I., Matsuda, Z., Taniguchi, T., and Shizuta, Y. Poly(ADP-ribose) synthetase. Separation and identification of three proteolytic fragments as the substrate-binding domain, the DNA-binding domain, and the automodification domain. J. Biol. Chem., *259:* 4770–4776, 1984.

2. Smith, S. The world according to PARP. Trends Biochem. Sci., *26:* 174–179, 2001.

3. Shall, S., and de Murcia, G. Poly(ADP-ribose) polymerase-1: what have we learned from the deficient mouse model? Mutat. Res., *460:* 1–15, 2000.

4. Ruf, A., Rolli, V., De Murcia, G., and Schulz, G. E. The mechanism of the elongation and branching reaction of Poly(ADP-ribose) polymerase as derived from crystal structures and mutagenesis. J. Mol. Biol., *278:* 57–65, 1998.

5. Lautier, D., Lagueux, J., Thibodeau, J., Menard, L., and Poirier, G. G. Molecular and biochemical features of poly (ADP-ribose) metabolism. Mol. Cell. Biochem., *122:* 171–193, 1993.

6. De Murcia, G., and Josiane Murcia, M. D. Poly(ADP-ribose) polymerase: A molecular nick-sensor. Trends Biochem. Sci., *19:* 172–176, 1994.

7. Lindahl, T., Satoh, M. S., Poirier, G. G., and Klungland, A. Post-translational modification of poly(ADP-ribose) polymerase induced by DNA strand breaks. Trends Biochem. Sci., *20:* 405–411, 1995.

8. Miwa, M., and Sugimura, T. Splitting of the ribose-ribose linkage of poly(adenosine diphosphate-robose) by a calf thymus extract. J. Biol. Chem., *246:* 6362–6364, 1971.

9. Alvarez-Gonzalez, R., and Althaus, F. R. Poly(ADP-ribose) catabolism in mammalian cells exposed to DNA-damaging agents. Mutat. Res., *218:* 67–74, 1989.

10. Berger, N. A. Poly(ADP-ribose) in the cellular response to DNA damage. Radiat. Res., *101:* 4–15, 1985.

11. Boulton, S., Pemberton, L. C., Porteous, J. K., Curtin, N. J., Griffin, R. J., Golding, B. T., and Durkacz, B. W. Potentiation of temozolomide-induced cytotoxicity: a comparative study of the biological effects of poly(ADP-ribose) polymerase inhibitors. Br. J. Cancer, *72:* 849–856, 1995.

12. Trucco, C., Oliver, F. J., de Murcia, G., and Menissier-de Murcia, J. DNA repair defect in poly(ADP-ribose) polymerase-deficient cell lines. Nucleic Acids Res., *26:* 2644–2649, 1998.

13. Agarwal, M. L., Agarwal, A., Taylor, W. R., Wang, Z. Q., Wagner, E. F., and Stark, G. R. Defective induction but normal activation and function of p53 in mouse cells lacking poly-ADP-ribose polymerase. Oncogene, *15:* 1035–1041, 1997.

14. Malanga, M., Pleschke, J. M., Kleczkowska, H. E., and Althaus, F. R. Poly(ADP-ribose) binds to specific domains of p53 and alters its DNA binding functions. J. Biol. Chem., *273:* 11839–43, 1998.

15. Pieper, A. A., Verma, A., Zhang, J., and Snyder, S. H. Poly (ADP-ribose) polymerase, nitric oxide and cell death. Trends Pharmacol. Sci., *20:* 171–181, 1999.

16. Yu, S. W., Wang, H. M., Poitras, M. F., Coombs, C., Bowers, W. J., Federoff, H. J., Poirier, G. G., Dawson, T. M., and Dawson, V. L. Mediation of poly(ADP-ribose) polymerase-1 dependent cell death by apoptosis-inducing factor. Science (Wash. DC), *297:* 259–263, 2002.

17. Dantzer, F., Schreiber, V., Niedergang, C., Trucco, C., Flatter, E., De La Rubia, G., Oliver, J., Rolli, V., Menissier-de Murcia, J., and De Murcia, G. Involvement of poly(ADP-ribose) polymerase in base excision repair. Biochimie, *81:* 69–75, 1999.

18. Wang, Z. Q., Auer, B., Stingl, L., Berghammer, H., Haidacher, D., Schweiger, M., and Wagner, E. F. Mice lacking ADPRT and poly(ADP-ribosyl)ation develop normally but are susceptible to skin disease. Genes Dev., *9:* 509–520, 1995.

19. Menissier-de Murcia, J., Niedergang, C., Trucco, C., Ricoul, M., Dutrillaux, B., Mark, M., Oliver, F. J., Masson, M., Dierich, A., LeMeur, M., Walztinger, C., Chambon, P., and de Murcia, G. Requirement of poly(ADP-ribose) polymerase in recovery from DNA damage in mice and in cells. Proc. Natl. Acad. Sci. USA., *94:* 7303–7307, 1997.

20. Masutani, M., Nozaki, T., Nishiyama, E., Shimokawa, T., Tachi, Y., Suzuki, H., Nakagama, H., Wakabayashi, K., and Sugimura, T. Function of poly(ADP-ribose) polymerase in response to DNA damage: gene-disruption study in mice. Mol. Cell. Biochem., *193:* 149–152, 1999.

21. Masutani, M., Suzuki, H., Kamada, N., Watanabe, M., Ueda, O., Nozaki, T., Jishage, K., Watanabe, T., Sugimoto, T., Nakagama, H., Ochiya, T., and Sugimura, T. Poly(ADP-ribose) polymerase gene disruption conferred mice resistant to streptozotocin-induced diabetes. Proc. Natl. Acad. Sci. USA, *96:* 2301–2304, 1999.

22. Hans, M. A., Muller, M., Meyer-Ficca, M., Burkle, A., and Kupper, J. H. Overexpression of dominant negative PARP interferes with tumor formation of HeLa cells in nude mice: Evidence for increased tumor cell apoptosis *in vivo*. Oncogene, *18:* 7010–7015, 1999.

23. Kupper, J. H., de Murcia, G., and Burkle, A. Inhibition of poly-(ADP-ribosyl)ation by overexpressing the poly(ADP-ribose) polymerase DNA-binding domain in mammalian cells. J. Biol. Chem., *265:* 18721–4, 1990.

24. Kupper, J. H., Muller, M., Jacobson, M. K., Tatsumi-Miyajima, J., Coyle, D. L., Jacobson, E. L., and Burkle, A. *trans*-dominant inhibition of poly(ADP-ribosyl)ation sensitizes cells against γ-irradiation and N-methyl-N′-nitro-N-nitrosoguanidine but does not limit DNA replication of a polyomavirus replicon. Mol. Cell. Biol., *15:* 3154–3163, 1995.

25. Molinete, M., Vermeulen, W., Burkle, A., Menissier-de Murcia, J., Kupper, J. H., Hoeijmakers, J. H., and de Murcia, G. Overproduction of the poly(ADP-ribose) polymerase DNA-binding domain blocks alkylation-induced DNA repair synthesis in mammalian cells. EMBO J., *12:* 2109–2117, 1993.

26. Schreiber, V., Hunting, D., Trucco, C., Gowans, B., Grunwald, D., De Murcia, G., and De Murcia, J. M. A dominant-negative mutant of human poly(ADP-ribose) polymerase affects cell recovery, apoptosis, and sister chromatid exchange following DNA damage. Proc. Natl. Acad. Sci. USA, *92:* 4753–4757, 1995.

27. Griffin, R. J., Curtin, N. J., Newell, D. R., Golding, B. T., Durkacz, B. W., and Calvert, A. H. The role of inhibitors of poly(ADP-ribose) polymerase as resistance-modifying agents in cancer therapy. Biochimie, *77:* 408–422, 1995.

28. Curtin, N. J., Golding, B. T., Griffin, R. J., Newell, D. R., Roberts, M. J., Srinivasan, S., and White, A. W. New PARP inhibitors for chemo- and radio-therapy of cancer. *In:* G. de Murcia and S. Shall (eds.), From DNA Damage and Stress Signalling to Cell Death: Poly

ADP-Ribosylation Reactions, pp. 177–206. Oxford, New York: Oxford University Press, 2000.

29. Durkacz, B. W., Omidiji, O., Gray, D. A., and Shall, S. (ADP-ribose)*n* participates in DNA excision repair. Nature (Lond.), *283:* 593–596, 1980.

30. Purnell, M. R., and Whish, W. J. Novel inhibitors of poly(ADP-ribose) synthetase. Biochem. J., *185:* 775–777, 1980.

31. Sestili, P., Spadoni, G., Balsamini, C., Scovassi, I., Cattabeni, F., Duranti, E., Cantoni, O., Higgins, D., and Thomson, C. Structural requirements for inhibitors of poly(ADP-ribose) polymerase. J. Cancer Res. Clin. Oncol., *116:* 615–622, 1990.

32. Suto, M. J., Turner, W. R., Arundel-Suto, C. M., Werbel, L. M., and Sebolt-Leopold, J. S. Dihydroisoquinolinones: The design and synthesis of a new series of potent inhibitors of poly(ADP-ribose) polymerase. Anti-Cancer Drug Des., *6:* 107–117, 1991.

33. Delaney, C. A., Wang, L. Z., Kyle, S., White, A. W., Calvert, A. H., Curtin, N. J., Durkacz, B. W., Hostomsky, Z., and Newell, D. R. Potentiation of temozolomide and topotecan growth inhibition and cytotoxicity by novel poly(adenosine diphosphoribose) polymerase inhibitors in a panel of human tumor cell lines. Clin. Cancer Res., *6:* 2860–2867, 2000.

34. Leopold, W., and Sebolt-Leopold, J. S. Chemical approaches to improve radiotherapy. *In:* F. A. Valeriote, T. H. Corbett, and L. H. Baker (eds.), Cytotoxic Anticancer Drugs: Models and Concepts for Drug Discovery and Development, pp. 179–196. Boston: Kluwer Academic Publishers, 1992.

35. Suto, M. J., and Suto, C. M. Inhibitors of poly(ADP-ribose) polymerase (ADPRP): Potential chemotherapeutic agents. Drugs Future, *16:* 723–739, 1991.

36. Ruf, A., De Murcia, G., and Schulz, G. E. Inhibitor and NAD+ binding to poly(ADP-ribose) polymerase as derived from crystal structures and homology modeling. Biochemistry, *37:* 3893–3900, 1998.

37. Almassy, R., Bowman, K., Calvert, A. H., Curtin, N. J., Golding, B. T., Hostomska, Z., Hostomsky, Z., Griffin, R. J., Maegley, K., Newell, D. R., Srinivasan, S., and Webber, S. The identification of novel potent 2-phenylbenzimidazole-4-carboxamide inhibitors of poly(ADP-ribose) polymerase (PARP). Proc. Am. Assoc. Cancer Res., *39:* 222, 1998.

38. White, A. W., Almassy, R., Calvert, A. H., Curtin, N. J., Griffin, R. J., Hostomsky, Z., Maegley, K., Newell, D. R., Srinivasan, S., and Golding, B. T. Resistance-modifying agents. 9. Synthesis and biological properties of benzimidazole inhibitors of the DNA repair enzyme poly(ADP-ribose) polymerase, J. Med. Chem., *43:* 4084–4097, 2000.

39. Canan Koch, S. S., Thoresen, L. H., Tikhe, J. G., Maegley, K. A., Almassy, R. A., Li, J., Yu, X-H., Zook, S. E., Kumpf, R. A., Zhang, C., Boritzki, T. J., Mansour, R. N., Zhang, K. E., Calabrese, C. R., Curtin, N. J., Kyle, S., Thomas, H. D., Wang, L. Z., Calvert, A. H., Golding, B. T., Griffin, R. J., Newell, D. R., Webber, S. E., and Hostomsky, Z. Novel tricyclic poly(ADP-ribose) polymerase-1 inhibitors with potent anticancer chemopotentiating activity: design, synthesis and X-ray co-crystal structure. J. Med. Chem., *45:* 4961–4974, 2002.

40. Marsischky, G. T., Wilson, B. A., and Collier, R. J. Role of glutamic acid 988 of human poly-ADP-ribose polymerase in polymer formation. J. Biol. Chem., *270:* 3247–3254, 1995.

41. Chen, T. R. *In situ* detection of mycoplasma contamination in cell cultures by fluorescent Hoechst 33258 stain. Exp. Cell Res., *104:* 255–262, 1977.

42. Skehan, P., Storeng, R., Scudiero, D., Monks, A., McMahon, J., Vistica, D., Warren, J. T., Bokesch, H., Kenney, S., and Boyd, M. R. New colorimetric cytotoxicity assay for anticancer-drug screening. J. Natl. Cancer Inst., *82:* 1107–1112, 1990.

43. Jacobson, E. L., and Jacobson, M. K. Tissue NAD as a biochemical measure of niacin status in humans, Methods Enzymol., *280:* 221–230, 1997.

44. Potter, G. W. H. Analysis of Biological Molecules: An Introduction to Principles, Instrumentation, and Techniques, 1st Ed., pp. 202. London: Chapman and Hall, 1995.

45. Tentori, L., Portarena, I., and Graziani, G. Potential clinical applications of poly(ADP-ribose) polymerase (PARP) inhibitors. Pharmacol. Res., *45:* 73–85, 2002.

46. Curtin, N. J., Barton, S., Batey, M. A., Calabrese, C. R., Calvert, A. H., Durkacz, B. W., Griffin, R. G., Golding, B. T., Kyle, S., Newell, D. R., Thomas, H. D., Wang, L-Z., Almassy, R., Boritzki, T., Canan-Koch, S., Hostomsky, Z., Maegley, K., and Webber, S. E. Anti-cancer chemosensitization *in vitro* and *in vivo* by a novel potent poly(ADP-ribose) polymerase (PARP-1) inhibitor. TBI-361. Clin. Cancer Res., *7:* 88, 2001.

Clinical Cancer Research

Identification of Potent Nontoxic Poly(ADP-Ribose) Polymerase-1 Inhibitors: Chemopotentiation and Pharmacological Studies

Christopher R. Calabrese, Michael A. Batey, Huw D. Thomas, et al.

Clin Cancer Res 2003;9:2711-2718.